TELKOMNIKA Indonesian Journal of Electrical Engineering
Vol. 14, No. 1, April 2015, pp. 24 ~ 33
DOI: 10.11591/telkomnika.v14i1.7650

Control and Modeling of PV–Wind Hybrid Energy Sources for Desalination System

Heba S. Abd-El Mageed*[1], Hanaa M. Farghally[1], Faten H. Fahmy[1], Mohamed A. Abuo Elmagd[2]
[1]PV Department, Electronics Research Institute, Cairo University, El Behous St, Giza, Egypt
[2]Faculty of engineering, Cairo University, El Behous St, Giza, Egypt
*Corresponding author, email: hebasa2008@yahoo.com

Abstract

Hybrid renewable energy based on PV and wind systems complemented with battery storage system are starting to play a vital role over the world to supply power to distant regions. This paper proposes the combination of lead acid battery system with a typical hybrid PV-wind energy system for supplying the electrical load of a desalination system at Mersa Matrouh. Solar and wind are sources of energy and battery unit is considered as a storage unit to meet the load demand. Simulation model with MATLAB/Simulink for the hybrid power system has been developed considering power supply variation in solar and wind hybrid power system caused due to disturbed power supply from wind turbine generator and solar system. A control strategy using Neural Network Control (NNC) is being offered and analyzed. The final result of the simulation indicates an effective operation of battery.

Keywords*: solar photovoltaic, wind power, battery energy storage, reverse osmosis system, artificial neural network*

1. Introduction

Out of the renewable energy resources such as wind, geothermal, solar, ocean, biomass and chemical resources, the wind and solar resources have its progress owing to its reliability, easiness etc. Due to the recurrent variant in the availability of these resources, the hybrid concept for power generation gains importance. Solar and wind power is a vast renewable energy source and they are widely available which has the good application prospect in terms of advance. The rational allocation of capacity for wind solar hybrid power system can increase reliability of power supply and decrease the system cost according to load characteristics of residential use and local environment condition [1].

For Hybrid Renewable Energy System (HRES) lead-acid batteries play a vital role as an energy storage unit. Even though batteries are the weaker section in the whole system, they are in need of certain initial investment of equipment. As the management of charging/discharging in storage battery directly affects the quality of power supply in Solar and Wind Hybrid Power system (SWHP) since electric energy from wind turbine generator and solar cells has observable fluctuation. It makes the system great demand to electric power management. Therefore, it is significant to study power management of batteries in detail [2].

In current days, artificial intelligence techniques are growing for the optimization and control of renewable power systems instead of conventional control and optimization methods. They are improving efficiency of renewable power generation.

The paper is organized as follows: firstly, presents the mathematical modeling of the PV Wind hybrid energy system. The NNC system is addressed secondly. And finally simulation results and conclusion are given.

2. Mathematical Modeling of Energy System

In this study, a hybrid energy generation system which includes wind, photovoltaic and battery is designed. A schematic diagram for PV- Wind hybrid energy system (HRES) powered desalination plant showed in Figure 1.

Received December 22, 2014; Revised March 2, 2015; Accepted March 18, 2015

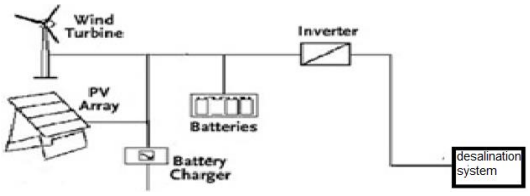

Figure 1. PV –Wind-Battery energy system

2.1. The Photovoltaic Model

The output current of the PV array consisting of several PV modules can be expressed as [3]:

$$I_p = MI_l - MI_o\left[exp\left(\frac{q\left(NV+\frac{I_pR_SN}{M}\right)}{NAKT_c}\right)-1\right]-\left[\frac{NV+\frac{IpRsN}{M}}{\frac{(NRsh)}{M}}\right] \quad (1)$$

Where Ip is output current of panel (A), Il is light generated current per module (A), Io is reverse saturation current per module (A), M is number of module strings in parallel, N is number of modules in each series string, V is terminal voltage for module (V), Rs is diode series resistance per module (ohms), Rsh is diode shunt resistance per module (ohms), Q is electric charge (1.6 × 10–19 C), K is the Boltzmann constant (1.38 × 10–23 J/K), A is diode ideality factor for the module, Tc is cell temperature (K).

The light-generated current equals to the short-circuit current (Il = Isc) [3].

$$I_l = P_lG[1 - P_2(G - G_r) + P_3(T_p - T_r))] \quad (2)$$

Where P1, P2, P3 is constant coefficients for Isc, Gr is reference solar irradiance (W/m2), G is solar irradiance (W/m2), Tr is reference temperature (K).Normally, 1000 W/m2 and 298 K are selected as the reference solar irradiance and reference temperature, respectively.

The reverse saturation current is [3]:

$$I_{o=BT_p{}^3}[exp(-\frac{E_{go}}{KT_p})] \quad (3)$$

Where Ego is band gap energy at 0 K (1.16 eV for silicon), B is a material constant.

The rate of change of Tc is suggested by [3]:

$$(mCp_{module})\frac{dT_c}{dt} = Q_{in} - Q_{rad} - Q_{conv} - Q_{elec} \quad (4)$$

Where mCp_{module} is effective thermal capacity of the PV module (J/K) at temperature Tc, Qin is solar energy absorbed by the module (W), Qrad is radiative heat loss (W), Qconv is convective heat loss (W) and Qelect is electrical power produced (W).

The solar energy absorbed by the photovoltaic module is expressed as [3]:

$$\mathrm{Q_{in}} = \propto_{abs} GS_p \quad (5)$$

Where $\propto_{abs} is$ overall absorption coefficient, Sp is total area of PV module (m2), G is global solar radiation on the PV module surface (W/m2).

The radiation heat loss is given by [3]:

$$Q_{\mathrm{radn}} = Q_{radn-ground}+Q_{radn-sky} \quad (6)$$

And,

$$Q_{radn-ground}=S_pF_{pg}\sigma\left(\varepsilon_{pT^4{}_c} - \varepsilon_{gT^4{}_g}\right) \quad (7)$$

$$Q_{adn-sky} = S_p F_{ps} \sigma(\varepsilon_p {T^4}_c - \varepsilon_s {T^4}_s) \quad (8)$$

Where σ is the Stephan-Boltzmann constant(5.67*10-8 w/m2K4), Fpg is panel-to-ground view factor, Fps is panel-to-sky view factor, εp is average emissivity of panel, εg is average emissivity of ground, εs is average emissivity of sky, Tg is ground temperature, Ts is sky temperature. Fps can be approximately taken to be equal to 1, Qradn-ground can be neglected, the values ofεp andεs of 0.88 and 1, respectively, the sky temperature is calculated from Ts=0.914Ta as suggested by [4].

The energy loss due to convection is given by the expression [3]:

$$Q_{conv} = S_p H(T_c - T_a) \quad (9)$$

Where H is the convective heat transfer coefficient for panel tilt angles less than 25 degrees and from low to moderate wind speed H is expressed as [3]:

$$H = 1.2475[\Delta T cos\beta]^{1/3} + 2.685\, V_{wind} \quad (10)$$

Where T is normal temperature difference (Tc–Ta), $\beta$is tilt angle (degrees) and Vwind is wind speed (m/s).

Electrical power produced is expressed as [3]:

$$Q_{elect} = \eta G S_c \quad (11)$$

Where η is module instantaneous efficiency, Sc is total surface area of PV cells.

The instantaneous efficiency is a function of the temperature of the module of the PV cell, that is:

$$\eta = \eta_0(1 - \gamma(T_c - T_r) \quad (12)$$

Where Tr is reference temperature (298 K), η_o is module efficiency at reference temperature, γ is coefficient for photovoltaic conversion efficiency.

Table 1 summarizes all parameters of the PV panel obtained directly from the manufacturer's specification sheet [3]:

Table 1. PV module coefficients used in the PV array model

Coefficient	Values
Series resistance (Rs)	2.28 ohms
Shunt resistance (Rsc)	250ohms
P1	4.1x10–3 m2/V
P2	–3.73x10–4 m2/W
P3	–2.44x10–3 K–1
Coefficient of Io (β)	7100 A/K3
Total surface area of PV module (Sp)	0.617 m2
Total surface area of cells in module (Sc)	0.5625 m2
Efficiency of module at reference temperature (η0)	12 %
Temperature coefficient (γ)	0.0045 K–1
Effective thermal capacity (mCp_{module})	9250 J/K
Overall absorption coefficient (αabs)	0.73

2.2. Wind Energy Conversion System Modeling

The wind turbine captures the wind's kinetic energy in a rotor consisting of two or more blades mechanically coupled to an electrical generator [5]. The equation describes the mechanical power captured from wind by a wind turbine can be formulated as [5]:

$$Pm=0.5\rho ACpv3 \quad (13)$$

Where ρ is Air density (Kg/m3), A is swept area (m2), Cp is Power coefficient of the wind turbine, V is Wind speed (m/s), t is Time (sec), the theoretical maximum value of the power coefficient Cp is 0.59.

TSR is defined as the linear speed of the rotor to the wind speed [5].

$$\mathrm{TSR} = \lambda = \frac{\omega \mathrm{R}}{\mathrm{V}} \quad (14)$$

Where ω is Turbine rotor speed (rad/s), R is Radius of the turbine blade (m), V is Wind speed (m/s) Based on equation (14) the optimum rotor speed can be estimated as follows [5]:

$$\omega_{opt} = \frac{TSR_{opt.}v}{R} \quad (15)$$

If Cp is known, the torque can be calculated from [5]:

$$T_a = \frac{1}{2}\rho A v^3 \frac{C_p}{\lambda} \quad (16)$$

Substituting (14) in (16), the torque can be written as: For below rated wind speed [5]:

$$T = k_{opt}.\omega^2 \quad (17)$$

Where:

$k_{opt} = \frac{1}{2}\rho A C_{p\,(}\frac{R}{\lambda})^3$ (18)

For above rated wind speed:

T= Prated /ω; for P≥ Prated

2.3. The Battery Storage Model

The battery bank, which is usually of the lead-acid type is used to store surplus electrical energy, to regulate system voltage and to supply power to load in case of low wind speed and/or low solar conditions. Lead-acid batteries used in hybrid systems operate under very specific conditions, and it is often very difficult to predict when energy will be extracted from or supplied to the battery. Most battery models mainly focus on three different characteristics, i.e. the battery state of charge (SOC) as well as the floating charge voltage (or the terminal voltage) and the battery lifetime. The battery model describing the relationship between the voltage, current and the state of charge is discussed [6].

$$V_B = V_r + I_B R_B \quad (19)$$

Where VB is Battery terminal voltage (V), IB is Battery current (A) (positive when charging and negative when discharging), Vr is Rest voltage (V), RB Is Internal resistance of the battery (ohms).

The rest voltage, Vr is expressed in terms of cell temperature as [6].

$$V_r = 2.04\left[1 - 0.001\left(T_c - T_r\right)\right] \quad (20)$$

The battery resistance during charge and discharge process is given by [6]:

$$R_{BC} = \frac{1}{BC}\left[R_i + \frac{0.189}{(1.142 - SOC)}\right] + (SOC - .9)\, ln\left(300\frac{I_B}{BC} + 1\right) \quad (21)$$

$$V_{bd} = V_r - \frac{1}{AH}\left(\frac{0.189}{SOC} + R_i\right) \quad (22)$$

$$R_{\,i} = 0.15\left[1 - 0.02\left(T_c - T_r\right)\right] \quad (23)$$

Where BC is Battery capacity, SOC is Battery state of charge. Tr is Reference temperature, Tc is Cell temperature.

The battery state of charge is [6]:

$$SOC = SOC_o + \frac{Q}{BC} \tag{24}$$

The exchanged charge can be determined by:

$$\mathrm{Q} = \int_0^t I_B \ \mathrm{dt} \tag{25}$$

Where SOC0 is Previous SOC, Q is Amount of exchanged charge from the previous time to the time of interest (C), BC is Battery capacity (Ah), BC is Battery capacity (Ah),IB is Battery current (A). The value of IB can be positive or negative depending on whether the battery is charging or discharging.

3. Seawater Reverse Osmosis (SWRO) System

In RO system, water is filtered through a membrane, leaving behind a large volume of water with high salt concentration that could be discarded outside the system.

The RO unit consists of a feed water source, pretreatment section, high pressure pump, membrane modules, and a post treatment. The two most basic individual components in SWRO system are the high-pressure feed pump and the RO membranes. These components comprise the heart of any RO system and require careful selection and application for successful operation, a schematic of the RO process is shown in Figure 2.

Pretreatment. The incoming feed water is pretreated to be compatible with the membranes by removing suspended solids, adjusting the pH, and adding a threshold inhibitor to control scaling caused by constituents such as calcium sulfate.

Pressurization. The pump raises the pressure of the pretreated feed water to an operating pressure appropriate for the membrane and the salinity of the feed water.

Separation. The permeable membranes inhibit the passage of dissolved salts while permitting the desalinated product water to pass through. The saline feed is pumped into a closed vessel where it is pressurized against the membrane. As a portion of the water passes through the membrane, the salt content in the remaining brine increases. At the same time, a portion of this brine is discharged without passing through the membrane.

Stabilization. The product water from the membrane assembly usually requires pH adjustment and degasification before being transferred to the distribution system for use as drinking water. The product passes through an aeration column in which the pH is elevated from a value of about 5 to close to 7. In many cases, this water is discharged to a storage cistern for later use [7].

A medium-size desalination RO plant with a capacity of 500m3/day is proposed to be installed in Mersa Matruh. The primary power-consuming device are the pump required to achieve the feed pressure needed to facilitate the reverse osmosis process.

An important consideration of any power generating system is load, SWRO load is assumed to work for 10 hours from 8:00 am to 18:00 pm, the measured annual average energy consumption has been considered to scale the load to 403 (kWh/d) in the present study.

The daily average load profile is shown in Figure 3. The peak requirements of the load in this study is 43.4 (kW) [8].

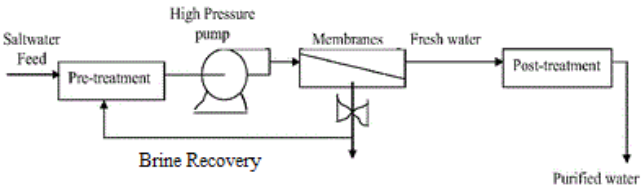

Figure 2. SWRO system

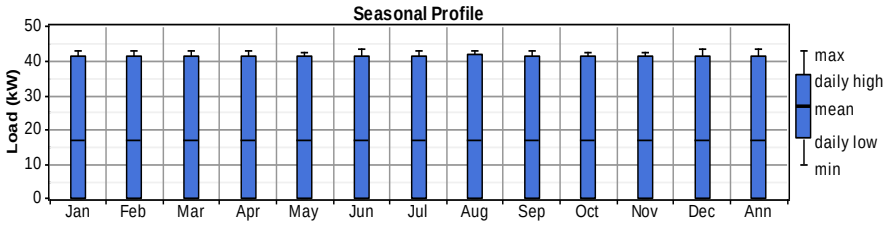

Figure 3. Monthly average load (kW) for a complete year

4. NN Control of Hybrid Energy System for Desalination System

Various types of controllers can be used to control MIMOs (multi inputs multi outputs system). One of the most precise and flexible controllers used for MIMOs is the neural network. Neural networks are controllers that approximately emulate the human neuron. Primarily, these networks were designed to model neural brain activity. However, as people began to recognize the advantages of neural networks, these networks were applied to controller algorithm design. Like a human neuron, neural networks work to store, analyze, and identify patterns in data by performing learning tasks. The ability of these networks to "learn" parallels the human neuron's ability to learn, making these automatic controllers the closest analog to a human controller [9], [10].

A schematic diagram of a neural network for the proposed hybrid energy system is shown in Figure 4. The NNC is used to control the charge/discharge operation of battery, the input layer is composed of four nodes in inputs which are: the solar radiation, the air temperature, the wind speed and the error data, the output layer is composed of one node that is the change of battery current Δ Ibattery.

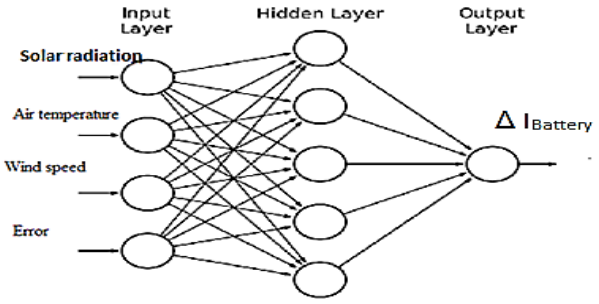

Figure 4. A schematic diagram of a neural network

5. Control Strategy of HRES

The proposed hybrid energy system is assumed to operate according to load following strategy. Under this strategy, only PV modules and wind turbines will charge the battery storage element. The PV/ Wind / Battery Hybrid Energy System with the associated NNC has different situations:

Firstly when Pg > PL, in this case The total power generated by the PV and Wind generators is greater than the power needed by the load, the energy surplus is stored in the batteries and the controller puts the battery in charge condition .When the battery capacity reaches a maximum value, the control system stops the charging process.

Secondly when Pg < PL, in this case the total PV and Wind generators power is less than the power needed by the load, the energy deficit is covered by the storage and the controller putts the battery in the discharge condition. If the battery capacity decreases to their minimum level, the control system disconnects the load and the energy deficit.

Thirdly when Pg = PL, The total power generated by the PV and Wind generators is equal to the power needed by the load. In this case the storage capacity remains unchanged.

6. Simulation Results

A series of simulation results are presented in this section. Fig. 5. Introduces a Simulink block diagram for the hybrid power system using MATLAB software.

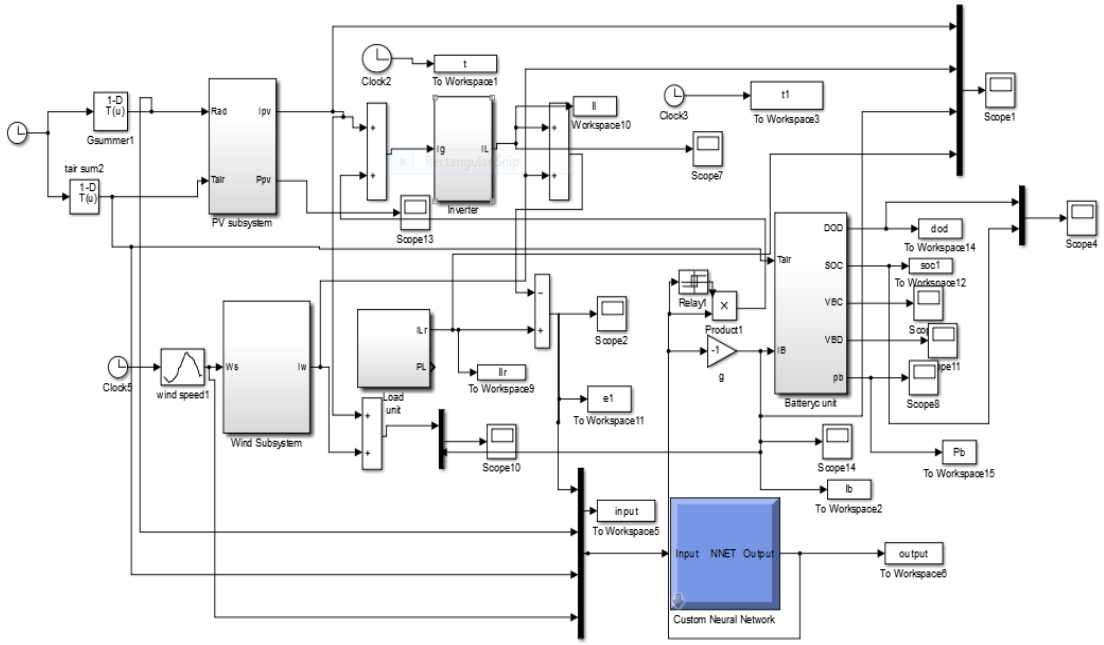

Figure 5. MATLAB Simulink diagram of power system

The following figures solar radiation, wind speed and air temperature data that are collected for summer and winter days.

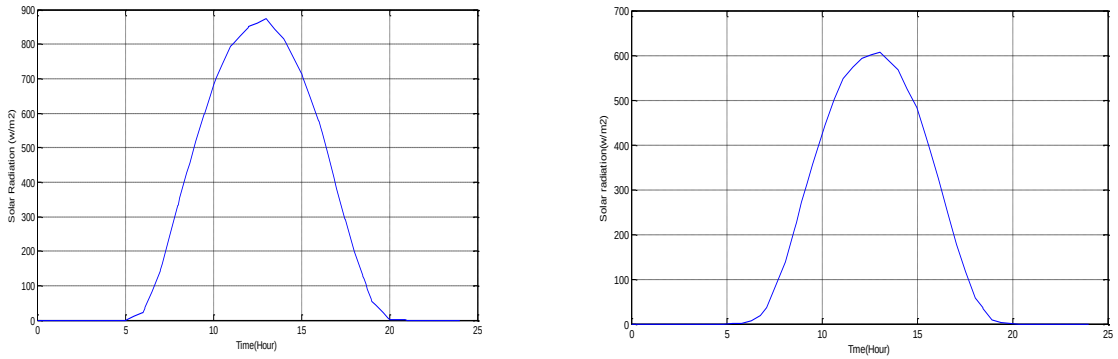

a) Summer b) Winter

Figure 6. Solar radiation data

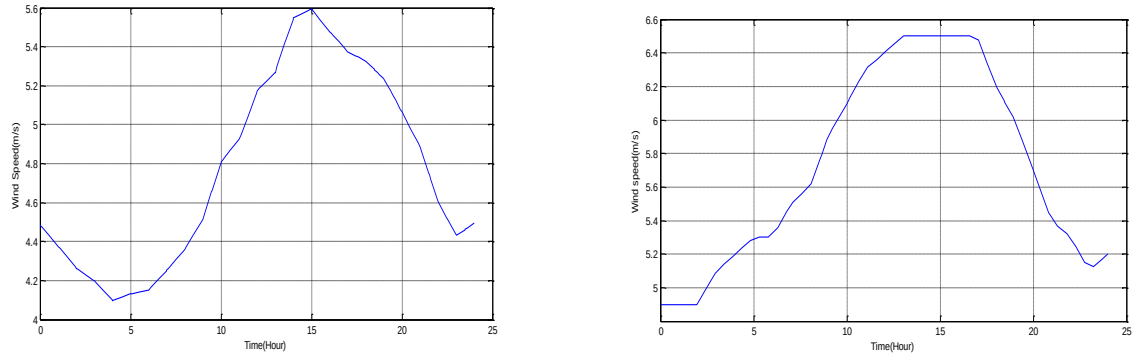

a) Summer *Winter*

Figure 7. Wind speed data (m/s)

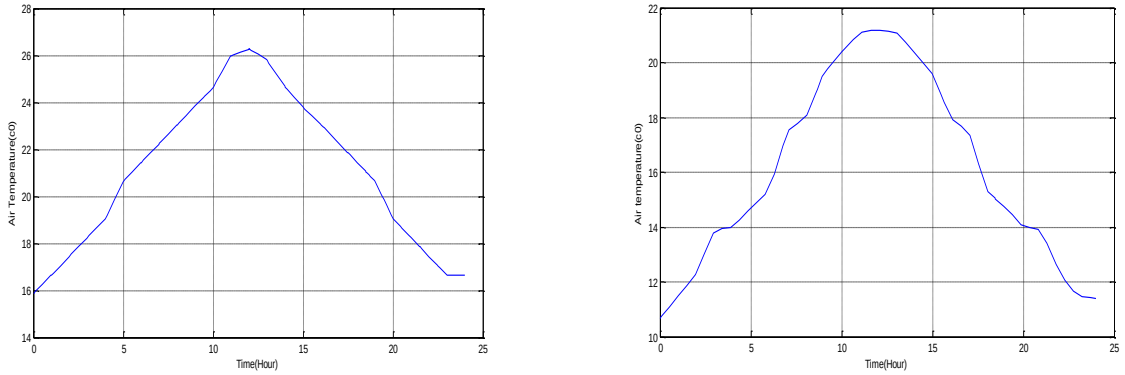

a)Summer b)Winter

Figure 8. Air temperature data (C^0)

As shown from the above Fig. 6 in summer, the radiation peaks at 11:30 am is about 850 W/m2. While in winter the radiation peaks of 600 W/m2 occurs at 12.30 pm. By comparing the winter & summer solar data, a wide range of radiation in summer than in winter. The wind speed changes randomly as indicated in Fig. 7, during summer the wind speed changes between 4 m/s to 5.6 m/s while in winter the variation of wind speed is between 4.9 m/s to 6.5 m/s. Fig. 8 shows the air temperature over 24 hours, the air temperature in the summer is higher than that in the winter.

Fig.9 introduces the load with PV- Wind generated current in summer and winter days, battery charge/discharge current in summer and winter days is illustrated in fig.10, as obvious from the figures that the simulation results are approximately similar during summer and winter days. During the night hours from, wind speed is high and solar radiation is only from 6am to 8 am and from7pm to 8pm, there is no load demand so the output current from PV generator and Wind generator must be stored and the battery in charging mode. In case of load working from 8am to 18 pm, periods from 8.5 am to 9.5 am and from 5pm to 6 pm, The generated current from the PV –Wind energy system cannot cover the load demand so the battery is in discharge mode but in period from 9.5 am to 1 pm, due to the high solar radiation, the generated current is higher than the load demand and the battery in charging mode.
Fig.11 showed that the error signal is approximately zero all the day hours during summer and winter seasons.

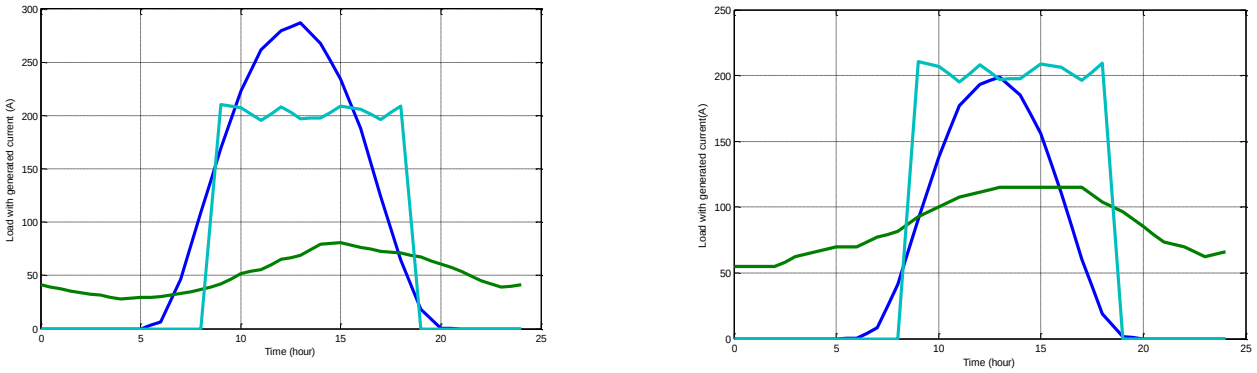

a) Summer b) Winter

Fig. 9 PV-Wind hybrid energy system output

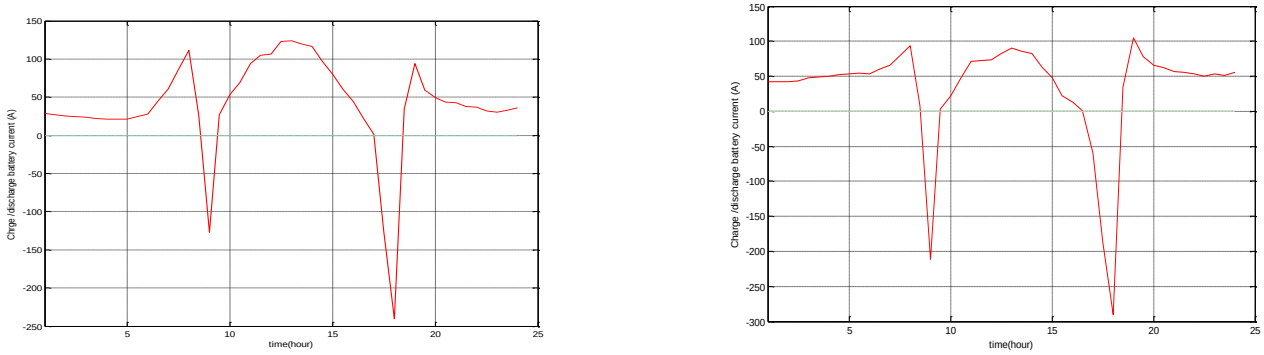

a) Summer b) Winter

Fig. 10 NNC output $\Delta I_{battery}$

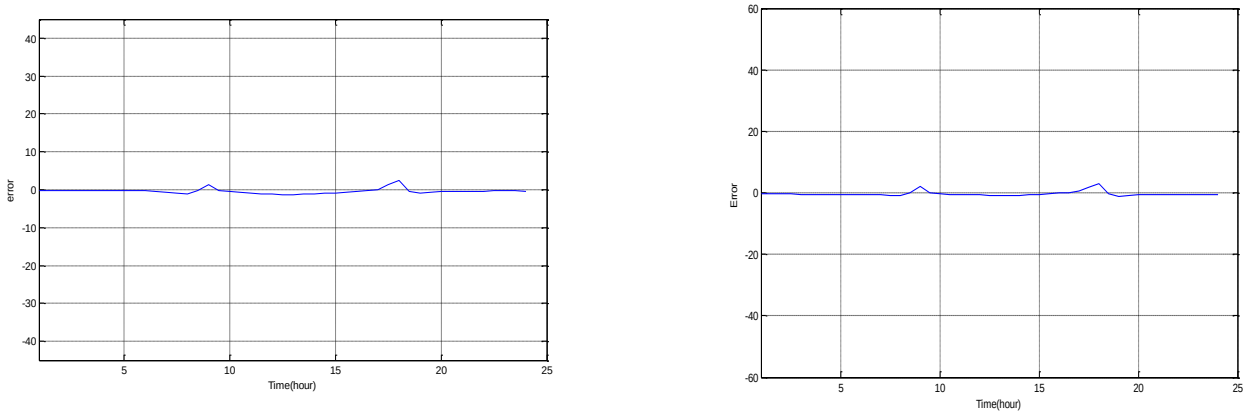

a) Summer b) Winter

Fig. 11 Error signal

6. Conclusion

This paper presented NNC technique to control PV-Wind hybrid system for feeding the electrical load of a desalination system at Mersa Matrouh zone in Egypt .Simulation studies have been carried out to verify the electrical performance in case of different scenarios using an estimated electrical desalination load profiles and real weather data of a Mersa Matruh. The results show that the overall power management strategy is effective and the power flows through the different energy sources and the load demand is balanced successfully in the electrical system. The results showed that the error signal is zero for long periods all the day during summer and winter. Simulation results achieved from MATLAB /Simulink shows the effectiveness of the good utilization of the battery with improved charging/discharging characteristic to meet the electrical load of a desalination system.

References

[1] SubyThomas, Kathirvel.C, "Operation and Control Strategy of Wind/Photovoltaic System with Battery Storage using Neural Networks", Transactions on Engineering and Sciences, December 2013, Vol. 1, PP. 13-18.
[2] P. Raju, Dr S. Vijayan, "Artificial Intelligence based Battery Power Management for Solar PV and Wind Hybrid Power System", International Journal of Engineering Research and General Science, December 2013, Vol. 1.
[3] Y. Sukamongkol, S. Chungpaibulpatana , W. Ongsakul ," A simulation model for predicting the performance of a solar photovoltaic system with alternating current loads", Renewable Energy ,2002,Vol.27,PP. 237-258.
[4] Rabl, Active solar collectors and their applications, Oxford University Press, USA (1985)
[5] Chaitanya Marisarla, K. Ravi Kumar, "A Hybrid Wind and Solar Energy System with Battery Energy Storage for an Isolated System", International Journal of Engineering and Innovative Technology (IJEIT), Vol. 3, PP. 99- 104, September 2013.
[6] Berndt D. Maintenance-free batteries. England: John Wiley & Sons. 1994.
[7] Ali Al-Karaghouli and Larry Kazmerski, "Economic and Technical Analysis of a Reverse-Osmosis Water Desalination Plant using DEEP-3.2 Software", Journal of Environmental Science & Engineering, Mar 2012, Vol. 1, PP. 318.
[8] Heba S. Abd-El Mageed, Hanaa M. Farghally, Faten H. Fahmy, Mohamed A. Abuo-Elmagd,**"** Optimal Sizing of Hybrid Renewable Energy System for Seawater Reverse Osmosis Desalination System", International Journal of Chemical and Environmental Engineering, Vol. 4, PP. 260- 265, August2013.
[9] Mei Shan Ngan, Chee Wei Tan, "Assessment of economic viability for PV/wind/diesel hybrid energy system in southern Peninsular Malaysia", Renewable and Sustainable Energy Reviews, 2012, PP. 634-647.
[10] MIMO Using Neural Networks, https://controls.engin.umich.edu/wiki/index.php/NN.